

1 **Quantifying SO₂ oxidation pathways to atmospheric sulfate by using**
2 **stable sulfur and oxygen isotopes: laboratory simulation and field**
3 **observation**

4 Ziyang Guo^a, Keding Lu^{a*}, Pengxiang Qiu^b, Mingyi Xu^b, Zhaobing Guo^{b*}
5

6 ^a State Key Joint Laboratory of Environmental Simulation and Pollution Control,
7 State Environmental Protection Key Laboratory of Atmospheric Ozone Pollution
8 Control, College of Environmental Sciences and Engineering, Peking University,
9 Beijing, China.

10 ^b Jiangsu Key Laboratory of Atmospheric Environment Monitoring and Pollution
11 Control (AEMPC), Collaborative Innovation Center of Atmospheric Environment and
12 Equipment Technology (CIC-AEET), School of Environmental Science and
13 Engineering, Nanjing University of Information Science and Technology, Nanjing
14 210044, China

15

16 * Correspondence to: k.lu@pku.edu.cn (Keding Lu), guocumt@nuist.edu.cn
17 (Zhaobing Guo)

18

19 **Abstract.** The formation of secondary sulfate in the atmosphere remains controversial, and it is urgent
20 to seek for a new method to quantify different sulfate formation pathways. Thus, SO₂ and PM_{2.5}
21 samples were collected from 4 to 22 Dec. 2019 in Nanjing region. Sulfur and oxygen isotopic
22 compositions were synchronously measured to study the contribution of SO₂ homogeneous and
23 heterogeneous oxidation to sulfate. Meanwhile, the correlation of δ¹⁸O values between H₂O and sulfate
24 from SO₂ oxidation by H₂O₂ and Fe³⁺/O₂ were simulatively investigated in the laboratory. Based on
25 isotope mass equilibrium equations, the ratios of different SO₂ oxidation pathways were quantified. The
26 results showed that secondary sulfate constituted higher than 80% of total sulfate in PM_{2.5} during the
27 sampling period. Laboratory simulation experiments indicated that δ¹⁸O value of sulfate was linearly
28 dependent on δ¹⁸O value of water, and the slopes of linear curves for SO₂ oxidation by H₂O₂ and
29 Fe³⁺/O₂ were 0.43 and 0.65, respectively. The secondary sulfate in PM_{2.5} was mainly ascribed to SO₂
30 homogeneous oxidation by OH radicals and heterogeneous oxidation by H₂O₂ and Fe³⁺/O₂. SO₂
31 heterogeneous oxidation was generally dominant during sulfate formation, and SO₂ oxidation by H₂O₂
32 predominated in SO₂ heterogeneous oxidation reactions with an average ratio around 54.6%. This study
33 provided an insight into precisely evaluating sulfate formation by combining stable sulfur and oxygen
34 isotopes.

35

36

37

38

39

40

41 **1 Introduction**

42 Sulfate is one of the prevalent components of PM_{2.5} (Brüggenmann et al., 2021; Huang et al., 2014;
43 Yang et al., 2023). Sulfate makes up approximately 25% of PM_{2.5} mass in Shanghai, 23% in
44 Guangzhou and 10-33% in Beijing (Xue et al., 2016). The rapid sulfate formation is a crucial factor
45 determining the explosive growth of fine particles and the frequent occurrence of severe haze events in
46 China (Lin et al., 2022; Liu et al., 2020; Meng et al., 2023; Wang et al., 2021). Sulfate plays an
47 important role in the chemical and physical processes in the troposphere and lower stratosphere, which
48 significantly affects global climate change by scattering solar radiation and acting as cloud
49 condensation nuclei (Gao et al., 2022; Ramanathan et al., 2001). Meanwhile, sulfate exerts a significant
50 influence on air quality and public health (Abbatt et al., 2006).

51 In the past decades, numerous attempts have been made to evaluate SO₂ oxidation pathways
52 involving in homogeneous and heterogeneous reactions. Traditionally, sulfate formation mechanisms
53 mainly include SO₂ homogeneous oxidation by OH radicals and heterogeneous oxidation by H₂O₂, O₃
54 and O₂ catalyzed by transition metal ions (TMIs) in cloud/fog water droplets. The relative importance
55 of different sulfate formation pathways is strongly dependent on oxidant concentrations, occurrence of
56 fog/cloud events and pH of aqueous phase (Kuang et al., 2022; Oh et al., 2023). Generally, SO₂
57 homogeneous oxidation by OH radicals and heterogeneous oxidation by H₂O₂ are considered the most
58 important pathways for sulfate production on the global scale (Seinfeld and Pandis, 1998). The
59 photochemical reactivity during the winter in Beijing has been found to be relatively high, which
60 favored the formation of reactive species such as OH radicals and H₂O₂, thereby facilitating SO₂
61 oxidation (Zhang et al., 2020). Xue et al. (2014) suggested that SO₂ oxidation by O₃ and H₂O₂ in
62 aqueous phase contributed to the majority of total sulfate production. Liu et al. (2020) proposed that
63 S(IV) oxidation by H₂O₂ in aerosol water could be an important pathway considering the ionic strength
64 effect. He et al. (2018) found that the contribution of SO₂ oxidation by H₂O₂ could reach 88% during
65 Beijing haze period. Ye et al. (2018) observed that SO₂ oxidation rate by H₂O₂ was 2-5 times faster
66 than the summed rate of the other three oxidation pathways. As a result, actual contribution of SO₂
67 oxidation by H₂O₂ during the winter might be underestimated in the previous studies.

68 In addition, the presence of NO₂ was obviously favorable for SO₂ oxidation under the conditions of
69 high relative humidity (RH) and NH₃. NH₃ can promote the hydrolysis of NO₂ dimers to HONO and

70 result in more sulfate formation on particle surface in humid conditions. However, this conclusion was
71 doubted by Liu et al. (2017) who believed that the reaction on actual fine particles with pH at 4.2 was
72 too slow to account for sulfate formation. Li et al. (2020) deemed that SO₂ oxidation by NO₂ might not
73 be a major oxidation pathway in China. Furthermore, GEOS-Chem modeling study suggested that NO₂
74 oxidation contributed less than 2% of total sulfate production. It is found that TMI pathway was very
75 important in highly polluted regions, and the contribution of metal-catalyzed SO₂ oxidation to sulfate
76 was as high as 49±10% in haze. Wang et al. (2021) also argued that SO₂ oxidation via TMI on aerosol
77 surface could be the dominant sulfate formation pathway. They found that manganese-catalyzed
78 oxidation of SO₂ contributed 69.2±5.0% in sulfate production. Overall, the mechanisms for sulfate
79 rapid growth remain unclear and controversial. Therefore, sulfate formation pathways need to be
80 further explored, and it is urgent to develop a new method to quantify different sulfate formation
81 processes.

82 Generally, sulfur isotopes allow for investigating SO₂ oxidation processes in the atmosphere because
83 of distinctive isotope fractionation associated with different oxidation reactions (Harris et al., 2013).
84 Harris et al. (2012) presented the respective sulfur isotope fractionation factors of SO₂ oxidation by OH,
85 O₃/H₂O₂ and iron catalysis. Besides, the observed sulfur isotope fractionation of SO₂ oxidation by H₂O₂
86 and O₃ appeared to be no significant difference. Therefore, the results were particularly useful to
87 determine the importance of transition metal-catalyzed oxidation pathway compared to other oxidation
88 pathways. However, other main SO₂ oxidation pathways could not be distinguished only based on
89 stable sulfur isotope determination.

90 Oxygen isotope ratio ($\delta^{18}\text{O}$) can be used to deduce sulfate formation processes due to those SO₂
91 oxidation pathways affect oxygen isotope of product sulfate differently. Especially, mass-independent
92 fractionation signals of oxygen isotopes (nonzero $\Delta^{17}\text{O}$, where $\Delta^{17}\text{O}=\delta^{18}\text{O}-0.52\times\delta^{17}\text{O}$) in sulfate are
93 usually adopted to investigate the contribution of different SO₂ oxidation pathways. This method can
94 identify the contribution of SO₂+O₃ pathway when high $\Delta^{17}\text{O}$ value (>3‰) is measured in sulfate.
95 However, there is presence of obvious uncertainty when interpreting the sulfate with low $\Delta^{17}\text{O}$ value
96 (<1‰). Unfortunately, most sulfate samples in the atmosphere present $\Delta^{17}\text{O}<1\text{‰}$, suggesting a limited
97 contribution of SO₂+O₃ pathway during sulfate formation. It is noteworthy that the contribution of
98 SO₂+H₂O₂ and TMI pathway is unclear if solely using $\Delta^{17}\text{O}$ (Li et al., 2020). Holt and Kumar (1984)

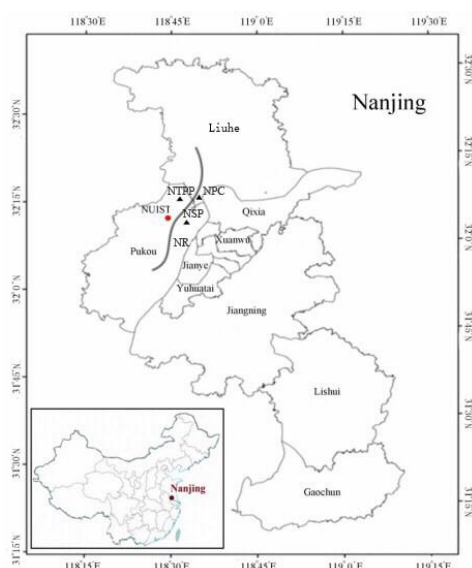
99 found oxygen isotope was a valuable and complementary method to determine probable mechanisms of
100 SO₂ oxidation to sulfate in the atmosphere. This provides us an insight into precisely evaluating sulfate
101 formation pathways by combining oxygen and sulfur isotopes.

102 In this contribution, PM_{2.5} and SO₂ were sampled from 4 to 22 Dec. 2019 in Nanjing. Sulfur and
103 oxygen isotopic compositions were measured to study the contribution of SO₂ homogeneous and
104 heterogeneous oxidation during sulfate formation. In addition, the linear relationships of δ¹⁸O values
105 between H₂O and sulfate from SO₂ oxidation by H₂O₂ and Fe³⁺/O₂ were synchronously investigated in
106 the laboratory. Based on sulfur and oxygen isotopes mass equilibrium equations, the ratios of different
107 SO₂ oxidation pathways during the sampling period were calculated. The study aims to seek for a novel
108 method to quantify different SO₂ oxidation processes with sulfur and oxygen isotopes.

109 2 Materials and methods

110 2.1 Sampling location

111 PM_{2.5} and SO₂ in the atmosphere were sampled from 4 to 22 Dec. 2019 in Nanjing, China. The
112 sampling site was located at the roof of the library in Nanjing University of Information Science &
113 Technology (NUIST, 32.1 °N, 118.5 °E), which is depicted in Fig. 1. The sampling location is at the
114 side of Ningliu Road and closely next to Nanjing chemical industry park. There is presence of some
115 large-scale chemical enterprises such as Nanjing steel plant, Nanjing thermal power plants and Nanjing
116 petrochemical company, which inevitably release lots of SO₂ and iron metal into the atmosphere.



117

118 Fig.1. Sampling site of NUIST in Nanjing, China. NSP: Nanjing steel plants; NTPP: Nanjing

119 thermal power plants; NPC: Nanjing petrochemical company; NR: Ningliu Road.

120 2.2 PM_{2.5} and SO₂ Samples collection

121 PM_{2.5} and SO₂ were sampled by using a modified JCH-1000 sampler (Jchuang Co., Qingdao) with
122 a flow rate of 1.05 m³ min⁻¹ from 8 am to 8 pm from 4 to 22 Dec. 2019. PM_{2.5} and SO₂ were collected
123 with quartz filter (203×254 mm, Munktell, Sweden) and glass fiber filter (203×254 mm, Tisch
124 Environment INC, USA), respectively. The filters were incinerated in a muffle furnace at 450 °C for 2h
125 and then preserved in the desiccators at room temperature. The glass fiber filters were firstly soaked in
126 2% K₂CO₃ and 2% glycerol solution for 2h and dried in DGG-9070A electric oven. SO₂ can be
127 changed into sulfite immediately during the sampling.

128 2.3 Extractions of water-soluble sulfate

129 PM_{2.5} sample filters were shredded and soaked in 400 mL of Milli-Q (18 MΩ) water for extractions
130 of water-soluble sulfate. Filters were then isolated from solutions by centrifugation and sulfate was
131 precipitated as BaSO₄ by adding 1 mol L⁻¹ BaCl₂. After the filtration with 0.22 μm acetate membrane,
132 BaSO₄ precipitate was rinsed with Milli-Q water to remove Cl⁻. Finally, BaSO₄ powders were calcined
133 at 800 °C for 2h to obtain high purity BaSO₄. In addition, a small amount of H₂O₂ solution was added
134 to oxidize sulfite to sulfate.

135 2.4 Laboratory simulation of SO₂ oxidation by H₂O₂ and Fe³⁺/O₂

136 For SO₂ oxidation by H₂O₂, 30 mL min⁻¹ Ar was firstly introduced into three kinds of different water
137 about 30 min to drive out air. Sulfate was produced by adding 10 mL H₂O₂ dilute solution (0.1 mL 30%
138 H₂O₂ in 50 mL water) to SO₂ in the reaction chamber at 10 °C. H₂O₂ solution was agitated vigorously
139 for 1min before admission of air. For SO₂ oxidation by Fe³⁺/O₂, 2 mL min⁻¹ SO₂ and 2 mL min⁻¹ O₂
140 were simultaneously put into Fe³⁺ dilute solution at 10 °C. Then, 10 mL 1 mL min⁻¹ BaCl₂ was added to
141 prepare BaSO₄. Oxygen isotopic compositions of product sulfate and three kinds of water were
142 measured to study their linear relationships.

143 2.5 Sulfur and oxygen isotope determination

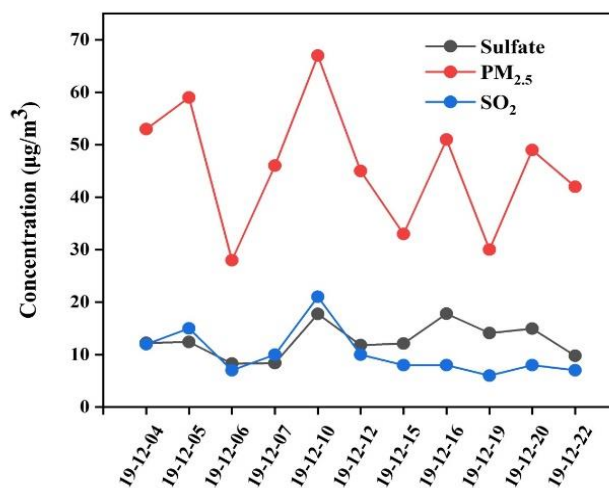
144 Sulfur isotopic compositions in sulfate were analyzed using Elemental analyzer (EA, Flash 2000,
145 Thermo) and isotope mass spectrometer (IRMS, Delta V Plus, Finningan). High-purity BaSO₄ was
146 converted into SO₂ in EA in the presence of Cu₂O. SO₂ from EA was ionized and δ³⁴S value was

147 measured using IRMS. For the determination of $\delta^{18}\text{O}$, BaSO_4 pyrolysis was conducted in graphite
148 furnace at 1450 °C, and $\delta^{18}\text{O}$ value was obtained in CO produced from the pyrolysis at continuous-flow
149 mode. The results of $\delta^{34}\text{S}$ and $\delta^{18}\text{O}$ were with respect to international standard V-CDT and V-SMOW,
150 and the accuracy were better than $\pm 0.2\%$ and $\pm 0.3\%$, respectively.

151 3 Results and discussion

152 3.1 Concentrations of $\text{PM}_{2.5}$, sulfate and SO_2

153 As described in Fig. 2, the mass concentrations of $\text{PM}_{2.5}$, SO_4^{2-} and SO_2 during the period from 4 to
154 22 Dec. 2019 in NUIST changed from 28.1 to 67.0 $\mu\text{g m}^{-3}$, 8.3 to 17.8 $\mu\text{g m}^{-3}$ and 6.2 to 20.9 $\mu\text{g m}^{-3}$
155 with an average and standard deviation at $45.7\pm 12.1 \mu\text{g m}^{-3}$, $12.7\pm 3.3 \mu\text{g m}^{-3}$ and $10.2\pm 4.4 \mu\text{g m}^{-3}$,
156 respectively. It can be observed that $\text{PM}_{2.5}$ average concentration was about 1.3 times of the First Grade
157 National Ambient Air Quality Standard ($35 \mu\text{g m}^{-3}$) and beyond the safety standard of World Health
158 Organization ($10 \mu\text{g m}^{-3}$). The photochemical reactivity during the winter in Beijing has been found to
159 be relatively high (Zhang et al., 2020), which facilitates the formation of some photooxidants. The
160 relatively clean days during the sampling period indicates the importance of photoinduced oxidation of
161 SO_2 .



162

163

Fig. 2. Variations in concentrations of $\text{PM}_{2.5}$, SO_4^{2-} and SO_2 .

164

165

166

Meanwhile, the change trends of $\text{PM}_{2.5}$, SO_4^{2-} and SO_2 concentrations were found to be basically the same during the sampling period, indicating sulfate was mainly from SO_2 oxidation. Especially, $\text{PM}_{2.5}$, SO_4^{2-} and SO_2 concentrations increased to the maximum values on 10 Dec.. It is noted that NO_2 and

167 CO concentrations were 85 and $1.60 \mu\text{g m}^{-3}$ on 10 Dec., which were also the maximum values during
168 the sampling period. Based on the wind speed was lower than 3m s^{-1} and there was presence of static
169 weather during the sampling period, we believed that high CO concentration was mainly from local
170 emissions. However, O_3 concentration on 10 Dec. was the minimum value at $24 \mu\text{g m}^{-3}$, which
171 preliminarily indicated that SO_2 oxidation by NO_2 might be a major pathway in sulfate formation.
172 Previous studies showed that SO_2 oxidation by NO_2 in aerosol water dominated heterogeneous sulfate
173 formation during wintertime at neutral aerosol pH (Wang et al., 2016; Cheng et al., 2016). However,
174 subsequent studies showed that the calculated aerosol pH was in the range of 4.2~4.7, and the
175 reactions between SO_2 and NO_2 during this pH range were too slow to produce sulfate. Taking into
176 account low aerosol pH in Nanjing region, we suggested that SO_2 oxidation by NO_2 was not a
177 dominant pathway for sulfate formation during the sampling period.

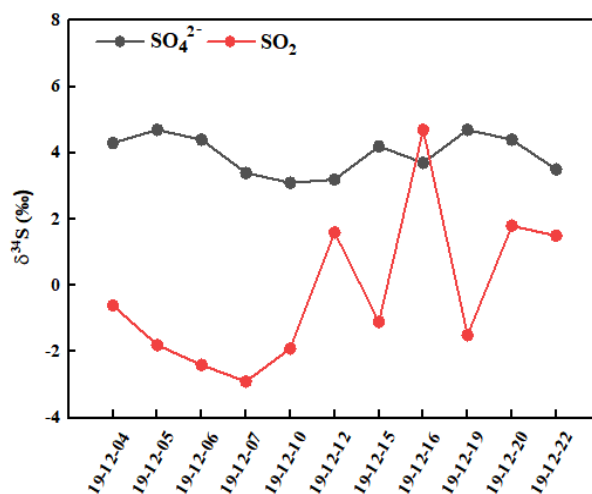
178 In contrast, $\text{PM}_{2.5}$, SO_4^{2-} and SO_2 concentrations were observed to be at the minimum values on 6
179 Dec.. Similarly, NO_2 and CO concentrations were also at the minimum of 36 and 0.6mg m^{-3} ,
180 respectively. However, O_3 concentration on 6 Dec. was the maximum at $50 \mu\text{g m}^{-3}$. Besides, the rate of
181 SO_2 oxidation with O_3 becomes fast only when $\text{pH}>5$, the reaction rate of SO_2 with O_3 is one hundredth
182 of those with H_2O_2 or TMI when $\text{pH}<5$. Therefore, pH values of actual fine particles at 4~5 in Nanjing
183 region could markedly restrain SO_2 oxidation by O_3 . The lowest SO_4^{2-} concentration on 6 Dec. further
184 demonstrated that SO_2 oxidation by O_3 played an insignificant role in sulfate formation.

185 Generally, aqueous-phase oxidation is deemed to be a main process of sulfate formation in
186 atmospheric environment. Shao et al. (2018) believed that heterogeneous sulfate production on aerosols
187 occurred when RH was higher than 50 %. The RH values of the atmosphere ranging from 50.7 to
188 88.9% during the sampling period indicated that sulfate formation was closely related to SO_2
189 heterogeneous oxidation.

190 3.2 Sulfur isotopic compositions in sulfate and SO_2

191 It can be observed from Fig. 3 that the values of $\delta^{34}\text{S-SO}_4^{2-}$ were generally higher compared to those
192 of $\delta^{34}\text{S-SO}_2$ during the sampling period except that on 16 Dec.. The $\delta^{34}\text{S-SO}_4^{2-}$ values ranged from 3.1
193 to 4.7‰ with an average and standard deviation at $4.0\pm 0.6\%$, while $\delta^{34}\text{S-SO}_2$ values changed from -2.9
194 to 4.7‰ with an average and standard deviation at $-0.2\pm 2.3\%$. The discrepancy between the values of
195 $\delta^{34}\text{S-SO}_4^{2-}$ and $\delta^{34}\text{S-SO}_2$ was mainly related to sulfur isotope fractionation effect during SO_2 oxidation

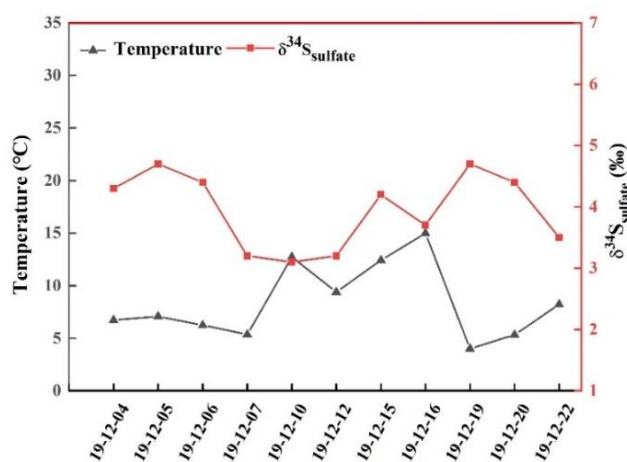
196 to secondary sulfate.



197
198 **Fig. 3.** Variations in sulfur isotopic compositions in sulfate and SO₂

199 It is noteworthy that $\delta^{34}\text{S-SO}_4^{2-}$ values were similar to that in PM_{2.5} with an average at 4.2‰ during
200 Youth Olympic Games in Aug. 2014 in Nanjing (Guo et al., 2016). However, the average value of
201 $\delta^{34}\text{S-SO}_4^{2-}$ during the sampling period was lower than 5.6‰ in Nanjing during a typical haze event
202 from 21 Dec. 2015 to 1 Jan. 2016 (Guo et al., 2019). The higher $\delta^{34}\text{S}$ values of sulfate in haze was
203 possibly ascribed to SO₂ heterogeneous oxidation, which typically enriched heavy sulfur isotope in
204 sulfate. In this study, the average concentrations of PM_{2.5} was 45.7 $\mu\text{g m}^{-3}$, indicating a not heavily
205 polluted time interval. Besides, the relatively high temperature during the sampling period was
206 favorable for photochemical reactions and OH radicals' formation. As a result, the contribution of SO₂
207 homogenous oxidation increased during sulfate formation, which enriched light sulfur isotope
208 compared to that in haze. Han et al. (2017) determined $\delta^{34}\text{S}$ values in Beijing PM_{2.5} with an average at
209 6.0‰. It is observed that there existed a regional difference in $\delta^{34}\text{S-SO}_4^{2-}$ values. The $\delta^{34}\text{S-SO}_4^{2-}$ value
210 in Nanjing was generally lower than that in Beijing. The discrepancy of $\delta^{34}\text{S-SO}_4^{2-}$ value illustrated
211 different sulfur sources and SO₂ oxidation pathways in these regions. In addition, $\delta^{34}\text{S-SO}_4^{2-}$ values
212 presented a seasonal change. $\delta^{34}\text{S}$ values in Beijing aerosol sulfate varied from 3.4 to 7.0‰ with an
213 average of 5.0‰ in summer and from 7.1 to 11.3‰ with an average of 8.6‰ in winter. Generally, SO₂
214 homogeneous oxidation dominated in summer compared to that in winter due to strong solar irradiation
215 (Han et al., 2016). SO₂ oxidation might lead to sulfur isotope fractionation, which was mainly
216 attributed to equilibrium or kinetic discrimination between SO₂ and sulfate. The influence of different
217 oxidants on sulfur isotope fractionation needed to be further investigated.

218 Fig.4 presents the relationship between $\delta^{34}\text{S}\text{-SO}_4^{2-}$ value and atmospheric temperature during the
 219 sampling period. It can be observed that there existed an obviously negative correlation. The higher
 220 temperature generally corresponded to the lower $\delta^{34}\text{S}\text{-SO}_4^{2-}$ value. This is mainly ascribed to kinetic
 221 effect of sulfur isotope fractionation during SO_2 oxidation. At high temperature, more OH radicals were
 222 produced and the contribution of SO_2 homogeneous oxidation increased. It is reported that sulfur
 223 isotope fractionation about SO_2 was -9‰ for homogeneous oxidation process (Tanaka et al., 1994).
 224 Therefore, low $\delta^{34}\text{S}$ value in sulfate at high temperature was chiefly due to elevated SO_2 homogeneous
 225 oxidation.



226

227 **Fig. 4.** The correlation between $\delta^{34}\text{S}\text{-SO}_4^{2-}$ value and atmospheric temperature.

228 3.3 Sulfur isotope fractionation during SO_2 oxidation

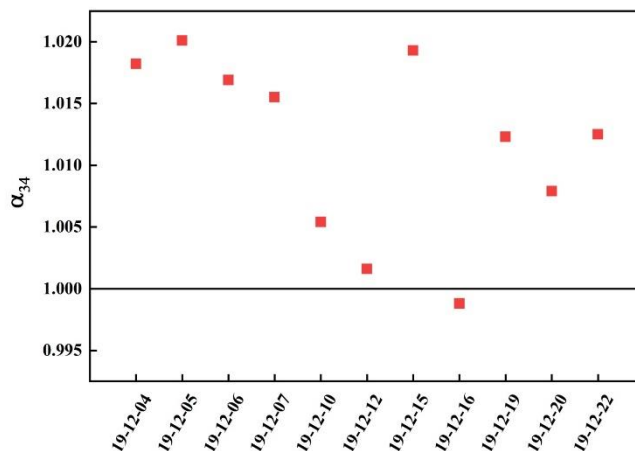
229 The secondary sulfate was generally from SO_2 homogeneous and heterogeneous oxidation (Seinfeld
 230 and Pandis, 1998). The homogeneous and heterogeneous oxidation of SO_2 might lead to sulfur isotope
 231 fractionation, which is described by using fractionation coefficient (α)

$$\alpha = \frac{\frac{\delta^{34}\text{S}_{\text{SO}_4^{2-}}}{10^3} + 1}{\frac{\delta^{34}\text{S}_{\text{SO}_2} + 1}{10^3}} \quad (1)$$

232

233 Sulfate enriched heavy sulfur isotope ($\alpha > 1$) during SO_2 heterogeneous oxidation for the presence of
 234 isotope equilibrium fractionation and kinetic fractionation. However, sulfate enriched light sulfur
 235 isotope ($\alpha < 1$) during SO_2 homogeneous oxidation due to this process was only related to kinetic
 236 fractionation. As described in Fig. 5, α values ranged from 0.9988 to 1.0201 indicating there existed
 237 SO_2 homogeneous and heterogeneous oxidation during the sampling period. α value was at the

238 minimum of 0.9988 on 16 Dec., which showed SO₂ homogeneous oxidation played a crucial role.



239

240

Fig. 5. Sulfur isotope fractionation coefficients during SO₂ oxidation.

241 It is reported that sulfur isotope fractionations during SO₂ heterogeneous and homogeneous oxidation
242 to sulfate were 16.5‰ and -9‰, respectively (Tanaka et al., 1994). Consequently, the contribution of
243 SO₂ heterogeneous and homogeneous oxidation to sulfate could be calculated by sulfur isotope mass
244 equilibrium equations (2) and (3).

$$245 \quad \delta^{34}\text{S}_{\text{SO}_2} + 16.5x - 9y = \delta^{34}\text{S}_{\text{SO}_4^{2-}} \quad (2)$$

$$246 \quad x + y = 1 \quad (3)$$

247 where x and y represent the contribution of SO₂ heterogeneous and homogeneous oxidation,
248 respectively.

249 It is observed from Fig. 6 that most of the days (7 out of 11) had more than 50% contributions from
250 SO₂ heterogeneous oxidation, which indicated that SO₂ heterogeneous oxidation was generally
251 dominant during sulfate formation. He et al. (2018) presented the observations of oxygen-17 excess of
252 PM_{2.5} sulfate collected in Beijing haze from Oct. 2014 to Jan. 2015, and found the contribution of
253 heterogeneous sulfate production was about 41~54% with a mean of 48±5%. The contribution of SO₂
254 heterogeneous oxidation reached high-level during 5-7 Dec. and on 19 Dec., which was closely related
255 to the temperature of the atmosphere. The low temperature about 5°C during these days was favorable
256 for SO₂ dissolution in water and further oxidized to sulfate. On 16 Dec., the contribution of SO₂
257 heterogeneous oxidation was at the minimum of 31.4%. The highest temperature of 15°C on 16 Dec.
258 restrained SO₂ solubility in aqueous solution and produced lots of gaseous oxidants such as OH
259 radicals to promote SO₂ homogeneous oxidation.

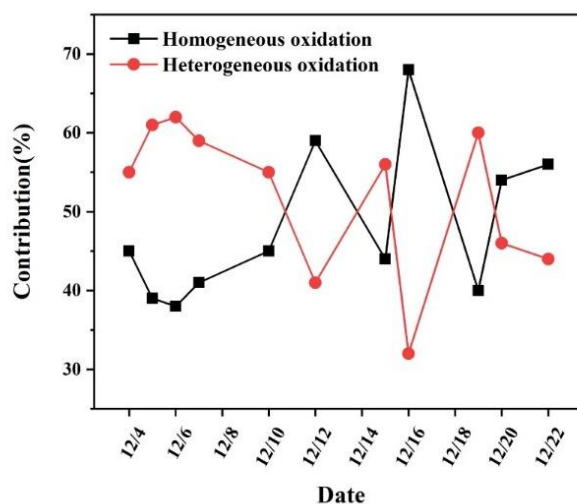


Fig. 6. The contributions of SO₂ heterogeneous and homogeneous oxidation to sulfate.

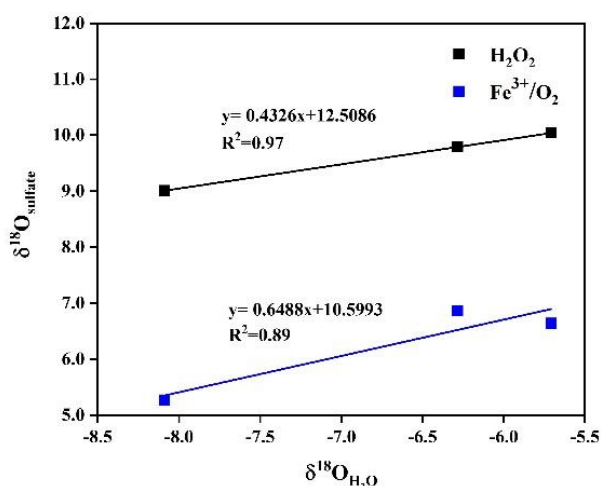
Overall, the temperature was an important factor in controlling SO₂ oxidation pathways. High temperature facilitated kinetic fractionation of sulfur isotope during SO₂ oxidation to sulfate, thereby decreasing $\delta^{34}\text{S}$ value in sulfate. In addition, there was lack of positive correlation between the contribution of SO₂ heterogeneous oxidation and O₃ or NO₂ concentration. This further demonstrated that SO₂ oxidation by O₃ and NO₂ were not the important pathways during the sampling period. Consequently, we mainly focused on SO₂ heterogeneous oxidation by H₂O₂ and Fe³⁺/O₂ in the following study.

3.4 The correlation of $\delta^{18}\text{O}$ values between H₂O and SO₄²⁻ from SO₂ oxidation by H₂O₂ and Fe³⁺/O₂

It is known that SO₂ rapidly equilibrates with ambient water for very high molar ratio of H₂O to SO₂ in the atmosphere. As a result, $\delta^{18}\text{O}$ value of SO₂ is dynamically controlled by $\delta^{18}\text{O}$ value of water and $\delta^{18}\text{O}$ value of SO₂ has no obvious effect on $\delta^{18}\text{O}$ value of sulfate produced from different oxidation pathways. Meanwhile, sulfate is very stable with respect to O atom exchange with ambient water. Consequently, $\delta^{18}\text{O}$ can be adopted to distinguish SO₂ oxidation processes due to that $\delta^{18}\text{O}$ value of product sulfate reflected the distinctive signals of different oxidants.

We simulatively studied SO₂ heterogeneous oxidation by H₂O₂ and Fe³⁺/O₂ in the laboratory, which aims to make clear the relationship of $\delta^{18}\text{O}$ values between product sulfate and three kinds of water at 10 °C. It can be observed from Fig. 7 that $\delta^{18}\text{O}$ value of sulfate was linearly dependent on $\delta^{18}\text{O}$ value of water, and the slope of linear curve for H₂O₂ oxidation approximates a ratio of 0.43, indicating that the isotopy of about two of four oxygen atoms in sulfate was controlled by $\delta^{18}\text{O}$ value of water. The other

281 two oxygen atoms were from H_2O_2 molecules, whose O-O bond remained intact during SO_2 oxidation.
 282 In addition, we noted from Fig. 7 that the slope of linear curve for $\text{Fe}^{3+}/\text{O}_2$ oxidation was about 0.65,
 283 which represented that the isotopy of about three of four oxygen atoms in sulfate was related to $\delta^{18}\text{O}$
 284 value of water. A 3/4 control of sulfate oxygens by water is also characteristic of heterogeneous
 285 oxidation mechanisms in which HSO_3^- isotopically equilibrated with water prior to significant
 286 oxidation to SO_4^{2-} . The other one oxygen atom in sulfate was from O_2 . The higher slope suggested a
 287 higher dependence of $\delta^{18}\text{O}$ value of sulfate on $\delta^{18}\text{O}$ value of water during SO_2 heterogeneous oxidation
 288 by $\text{Fe}^{3+}/\text{O}_2$. The discrepancy of the slopes for different SO_2 heterogeneous oxidation processes provides
 289 us a potential method to distinguish SO_2 oxidation pathways.



290
 291 **Fig.7.** The correlation of $\delta^{18}\text{O}$ values between H_2O and sulfate from SO_2 oxidation by H_2O_2 and
 292 $\text{Fe}^{3+}/\text{O}_2$, respectively.

293 3.5 $\delta^{18}\text{O}\text{-SO}_4^{2-}$ values in $\text{PM}_{2.5}$ and SO_2 main oxidation pathways

294 As depicted in Fig. 8, $\delta^{18}\text{O}$ values of sulfate in $\text{PM}_{2.5}$ ranged from 11.09 to 12.93‰ with an average
 295 and standard deviation of 12.35 ± 0.68 ‰. $\delta^{18}\text{O}$ values of sulfate focused on a narrow scope except those
 296 on 5 and 22 Dec.. It should be pointed out $\delta^{18}\text{O}$ value of secondary sulfate was a comprehensive result
 297 from different SO_2 oxidation processes. Sulfate in $\text{PM}_{2.5}$ usually consisted of primary sulfate and
 298 secondary sulfate. The $\delta^{18}\text{O}$ value of primary sulfate is about 38 ‰ (Holt and Kumar, 1984), which is
 299 significantly higher than those of secondary sulfate. The contribution of primary and secondary sulfate

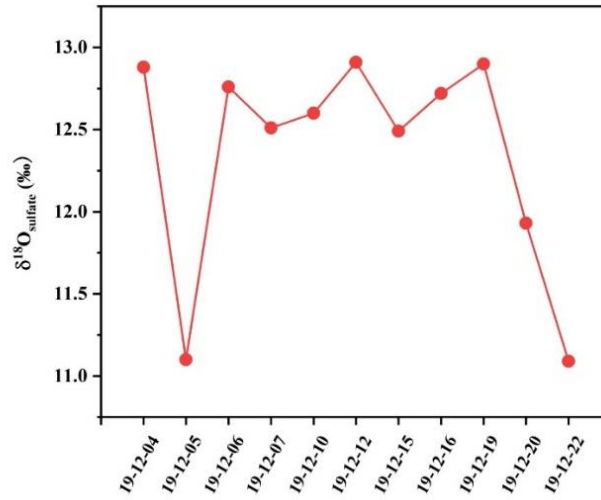


Fig.8. δ¹⁸O values of sulfate in PM_{2.5} during the sampling period.

in the atmosphere can be calculated by oxygen isotope mass equilibrium equation (4) (Ben et al., 1982).

$$\delta^{18}\text{O}_{\text{PM}_{2.5}} = \delta^{18}\text{O}_{\text{PS}} \times (1 - f_{\text{SS}}) + \delta^{18}\text{O}_{\text{SS}} \times f_{\text{SS}} \quad (4)$$

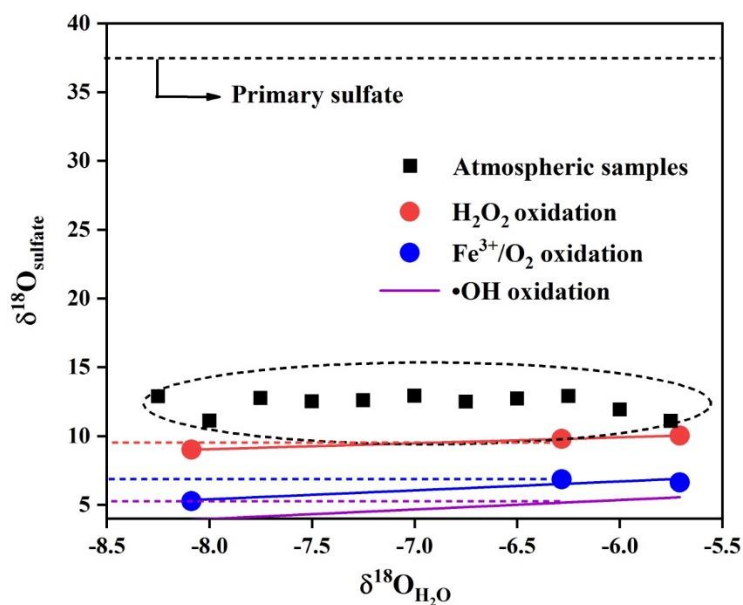
where δ¹⁸O_{PM_{2.5}}, δ¹⁸O_{PS} and δ¹⁸O_{SS} mean δ¹⁸O values of PM_{2.5}, primary sulfate and secondary sulfate, respectively; f_{SS} is the contribution of secondary sulfate in PM_{2.5}.

It is noteworthy from Fig. 9 that there exists a linear relationship between δ¹⁸O values in water and secondary sulfate from different SO₂ oxidation pathways, and this can be described by the equations (5)-(7), where the value of δ¹⁸O_{water} is about -6.2‰ in Nanjing. As discussed above, secondary sulfate was mainly ascribed to SO₂ homogeneous oxidation by OH radicals and heterogeneous oxidation by H₂O₂ and Fe³⁺/O₂. Therefore, δ¹⁸O_{SS} value in equation (4) can be obtained based on equations (5)-(7), respectively. As a result, the average contribution of primary and secondary sulfate in PM_{2.5} are presented in Table 1. It can be observed that the majority of sulfate in PM_{2.5} was secondary sulfate, which appears to constitute from 79.9 to 86.2% of total sulfate during the sampling period. It is admirable to quantitatively describe these formation pathways of secondary sulfate in PM_{2.5}.

$$\delta^{18}\text{O}_{\text{SS}} = 0.69 \times \delta^{18}\text{O}_{\text{water}} + 9.5 \text{ ‰ (OH) (Holt and Kumar, 1984)} \quad (5)$$

$$\delta^{18}\text{O}_{\text{SS}} = 0.65 \times \delta^{18}\text{O}_{\text{water}} + 10.6 \text{ ‰ (Fe}^{3+}/\text{O}_2\text{) (this study)} \quad (6)$$

$$\delta^{18}\text{O}_{\text{SS}} = 0.43 \times \delta^{18}\text{O}_{\text{water}} + 12.5 \text{ ‰ (H}_2\text{O}_2\text{) (this study)} \quad (7)$$



320

321

Fig.9. The correlation between $\delta^{18}\text{O}$ values in water and sulfate in $\text{PM}_{2.5}$.

322

Table 1 The average contribution of primary sulfate and secondary sulfate in $\text{PM}_{2.5}$.

Sampling time	Primary sulfate (%)	Secondary sulfate (%)
4 Dec.	19.7	80.3
5 Dec.	13.9	86.1
6 Dec.	19.3	80.7
7 Dec.	18.4	81.6
10 Dec.	18.7	81.3
12 Dec.	20.0	80.0
15 Dec.	18.4	81.6
16 Dec.	20.1	79.9
19 Dec.	19.7	80.3
20 Dec.	16.7	83.3
22 Dec.	13.8	86.2

323

324 According to the percentages of SO_2 heterogeneous and homogeneous oxidation to sulfate in Fig.6

325 and the average contributions of primary sulfate and secondary sulfate in $\text{PM}_{2.5}$ in Table 1, we can

326 further calculate the ratios of different SO_2 oxidation pathways at 10 °C via oxygen isotope mass

327 equilibrium equations (8)-(10), and the corresponding results are depicted in Table 2.

$$328 \quad \delta^{18}\text{O}_{\text{PM}_{2.5}} = \delta^{18}\text{O}_{\text{PS}} \times f_{\text{PS}} + (\delta^{18}\text{O}_{\text{SS-OH}} \times f_{\text{SS-OH}} + \delta^{18}\text{O}_{\text{SS-Fe}^{3+}/\text{O}_2} \times f_{\text{SS-Fe}^{3+}/\text{O}_2} + \delta^{18}\text{O}_{\text{SS-H}_2\text{O}_2} \times f_{\text{SS-H}_2\text{O}_2}) \times f_{\text{SS}} \quad (8)$$

$$329 \quad f_{\text{PS}} + f_{\text{SS}} = 1 \quad (9)$$

$$330 \quad f_{\text{SS-OH}} + f_{\text{SS-Fe}^{3+}/\text{O}_2} + f_{\text{SS-H}_2\text{O}_2} = 1 \quad (10)$$

331 where $\delta^{18}\text{O}_{\text{PM}_{2.5}}$ and $\delta^{18}\text{O}_{\text{PS}}$ are $\delta^{18}\text{O}$ values of total sulfate and primary sulfate in $\text{PM}_{2.5}$; $\delta^{18}\text{O}_{\text{SS-OH}}$,
 332 $\delta^{18}\text{O}_{\text{SS-Fe}^{3+}/\text{O}_2}$ and $\delta^{18}\text{O}_{\text{SS-H}_2\text{O}_2}$ are $\delta^{18}\text{O}$ values of secondary sulfate from SO_2 oxidation by OH radicals,
 333 $\text{Fe}^{3+}/\text{O}_2$ and H_2O_2 , respectively; f_{PS} and f_{SS} are the contribution of primary and secondary sulfate; $f_{\text{SS-OH}}$,
 334 $f_{\text{SS-Fe}^{3+}/\text{O}_2}$ and $f_{\text{SS-H}_2\text{O}_2}$ are the ratios of secondary sulfate from SO_2 oxidation by OH radicals, $\text{Fe}^{3+}/\text{O}_2$ and
 335 H_2O_2 , respectively.

336 Unlike heavily polluted days with reduced solar irradiation, the photochemical reactivity can remain
 337 high in clean days during the observation period because of relatively intense solar irradiation. As a
 338 result, some photochemical reactive species such as OH radicals and H_2O_2 are deemed to be the major
 339 oxidants for sulfate formation. Generally, H_2O_2 production in the relatively clean atmosphere is
 340 ascribed to self-reaction of HO_2 radicals that mainly come from the reactions of OH radicals with CO
 341 and volatile organic compounds. It is observed from Table 2 that the ratios of SO_2 oxidation by OH
 342 radicals ranged from 38 to 68% with an average and standard deviation at $48 \pm 9.7\%$. The ratio reached
 343 the maximum of 68% on 16 Dec., which is mainly ascribed to the highest temperature of 15°C during
 344 the sampling period. The photochemical reactions are favorable for producing more OH radicals. In
 345 contrast, the ratio of SO_2 oxidation by OH radicals decreased to the minimum of 38% on 6 Dec. due to
 346 the low temperature.

347 **Table 2** The ratios of SO_2 different oxidation pathways to sulfate.

Time	$f_{\text{SS-OH}}$	$f_{\text{SS-H}_2\text{O}_2}$	$f_{\text{SS-Fe}^{3+}/\text{O}_2}$	$f_{\text{SS-H}_2\text{O}_2} / (f_{\text{SS-H}_2\text{O}_2} + f_{\text{SS-Fe}^{3+}/\text{O}_2}) (\%)$
4 Dec.	0.45	0.27	0.28	49.1
5 Dec.	0.39	0.24	0.37	39.3
6 Dec.	0.38	0.24	0.38	38.7
7 Dec.	0.41	0.25	0.34	42.3
10 Dec.	0.45	0.27	0.28	49.1
12 Dec.	0.59	0.30	0.11	73.2
15 Dec.	0.44	0.26	0.30	46.5

16 Dec.	0.68	0.26	0.06	81.2
19 Dec.	0.40	0.25	0.35	41.6
20 Dec.	0.54	0.31	0.15	67.4
22 Dec.	0.56	0.32	0.12	72.7

348

349 It is known that SO₂ oxidation by H₂O₂ and Fe³⁺/O₂ are the most important pathways during SO₂
350 heterogeneous oxidation. It can be observed from table 2 that the percentage of sulfate from SO₂
351 oxidation by H₂O₂ in secondary sulfate from SO₂ heterogeneous oxidation changed from 38.7 to 81.2%
352 with an average and standard deviation at 54.6±15.7%, indicating that SO₂ oxidation by H₂O₂
353 predominated during SO₂ heterogeneous oxidation. In addition, there existed an obviously positive
354 correlation between the ratios of SO₂ oxidation by H₂O₂ and OH radicals, which was chiefly attributed
355 to the photochemical reactions. The relatively strong solar irradiation on 16 Dec. resulted in the
356 maximum ratio of 81.2% about H₂O₂ oxidation in SO₂ heterogeneous reactions. The sampling site is
357 close to Nanjing steel plant. As companion emitters, Fe³⁺ are present in much higher concentrations
358 than that in other areas. It is believed that SO₂ oxidation by O₂ in the presence of Fe³⁺ was not negligent
359 in the areas where the concentrations of SO₂ and Fe³⁺ were high. This inevitably resulted in high SO₂
360 oxidation ratio by Fe³⁺/O₂ in SO₂ heterogeneous oxidation processes.

361 4 Conclusions

362 There was no serious PM_{2.5} pollution during the sampling period. The secondary sulfate constitutes
363 from about 79.9 to 86.2% of total sulfate in PM_{2.5}. SO₂ oxidation by O₃ and NO₂ played an
364 insignificant role in sulfate formation. The secondary sulfate was mainly ascribed to SO₂ homogeneous
365 oxidation by OH radicals and heterogeneous oxidation by H₂O₂ and Fe³⁺/O₂. Compared to
366 homogeneous oxidation, SO₂ heterogeneous oxidation was generally dominant with an average
367 contribution of 51.6%. SO₂ oxidation by H₂O₂ predominated in SO₂ heterogeneous oxidation reactions
368 and the average ratio of which reached 54.6%. Consequently, sulfur and oxygen isotopes can be used to
369 gain an insight into sulfate formation. Sulfur isotopic compositions in SO₂ and sulfate were
370 simultaneously measured to quantify the contributions of SO₂ homogeneous and heterogeneous
371 oxidation. Combining field observations of oxygen isotope in the atmosphere with the linear
372 relationships of δ¹⁸O values between H₂O and sulfate from different SO₂ oxidation processes can obtain

373 an increased understanding of specific sulfate formation pathways. This study is favorable for deeply
374 investigating sulfur cycle in the atmosphere.

375

376 **Author contribution**

377 Ziyang Guo carried out the experiment and wrote the original draft. Keding Lu designed the
378 methodology and administrated the project. Pengxiang Qiu and Mingyi Xu performed the data
379 collection. Zhaobing Guo instructed the experiment and revised the paper.

380 **Competing interests**

381 The authors declare that they have no competing interest that can influence the work reported in this
382 paper.

383 **Acknowledgement**

384 We gratefully acknowledge the financial supports from the National Natural Science Foundation of
385 China (Nos. 41873016, 51908294, and 21976006), the National Science Fund for Distinguished Young
386 Scholars (No. 22325601).

387

388

389 **References**

- 390 Abbatt, J. P. D., Benz, S., Cziczo, D. J., Kanji, Z., Lohmann, U., and Mohler, O.: Solid ammonium
391 sulfate aerosols as ice nuclei: a pathway for cirrus cloud formation, *Science*, 313, 1770-1773,
392 <https://doi.org/10.1126/science.1129726>, 2006.
- 393 Ben, D. H., Romesh, K., and Paul, T. C.: Primary Sulfates in Atmospheric Sulfates: Estimation by
394 Oxygen Isotope Ratio Measurements, *Science*, 217, 51-53, <https://doi.org/10.1126/science.217.4554.51>,
395 1982.
- 396 Brüggemann, M., Riva, M., Perrier, S., Poulain, L., George, C., and Herrmann, H.: Overestimation of
397 Monoterpene Organosulfate Abundance in Aerosol Particles by Sampling in the Presence of SO₂,
398 *Environ. Sci. Technol. Lett.*, 8, 206-211, <https://doi.org/10.1021/acs.estlett.0c00814>, 2021.
- 399 Cheng, Y. F., Zheng, G. J., Wei, C., Mu, Q., Zheng, B., Wang, Z. B., Gao, M., Zhang, Q., He, K. B.,
400 Carmichael, G., Pöschl, U., and Su, H.: Reactive Nitrogen Chemistry in Aerosol Water as a Source of
401 Sulfate during Haze Events in China, *Sci. Adv.*, 2, e1601530, <https://doi.org/10.1126/sciadv.1601530>,
402 2016.
- 403 Gao, J., Wei, Y., Zhao, H., Liang, D., Feng, Y., and Shi, G.: The role of source emissions in sulfate
404 formation pathways based on chemical thermodynamics and kinetics model, *Sci. Total. Environ.*, 851,
405 158104, <https://doi.org/10.1016/j.scitotenv.2022.158104>, 2022.
- 406 Guo, Z. B., Shi, L., Chen, S. L., Jiang, W. J., Wei, Y., Rui, M. L., and Zeng, G.: Sulfur isotopic
407 fractionation and source apportionment of PM_{2.5} in Nanjing region around the second session of the
408 Youth Olympic Games, *Atmos. Res.*, 174-175, 9-17, <https://doi.org/10.1016/j.atmosres.2016.01.011>,
409 2016.
- 410 Guo, Z. Y., Guo, Q. J., Chen, S. L., Zhu, B., Zhang, Y., Yu, J., and Guo, Z. B.: Study on pollution
411 behavior and sulfate formation during the typical haze event in Nanjing with water soluble inorganic
412 ions and sulfur isotopes, *Atmos. Res.*, 217, 198-207, <https://doi.org/10.1016/j.atmosres.2018.11.009>,
413 2019.
- 414 Han, X. K., Guo, Q. J., Liu, C. Q., Fu, P. Q., Strauss, H., Yang, J., Jian, H., Wei, L., Hong, R., Peters,
415 M., Wei, R. F., and Tian, L.: Using stable isotopes to trace sources and formation processes of sulfate
416 aerosols from Beijing, China, *Sci. Rep.*, 6, 29958, <https://doi.org/10.1038/srep29958>, 2016.
- 417 Han, X. K., Guo, Q. J., Strauss, H., Liu, C. Q., Hu, J., Guo, Z. B., Wei, R. F., Peters, M., Tian, L., and

418 Kong, J.: Multiple Sulfur Isotope Constraints on Sources and Formation Processes of Sulfate in Beijing
419 PM_{2.5} Aerosol, *Environ. Sci. Technol.*, 51, 7794-7803, <https://doi.org/10.1021/acs.est.7b00280>, 2017.

420 Harris, E., Sinha, B., Hoppe, P., and Ono, S.: High-precision measurements of ³³S and ³⁴S fractionation
421 during SO₂ oxidation reveal causes of seasonality in SO₂ and sulfate isotopic composition, *Environ. Sci.*
422 *Technol.*, 47, 12174-12183, <https://doi.org/10.1021/es402824c>, 2013.

423 Harris, E., Sinha, B., Hoppe, P., Crowley, J. N., Ono, S., and Foley, S.: Sulfur isotope fractionation
424 during oxidation of sulfur dioxide: gas-phase oxidation by OH radicals and aqueous oxidation by H₂O₂,
425 O₃ and iron catalysis, *Atmos. Chem. Phys.*, 12, 407-424, <https://doi.org/10.5194/acp-12-407-2012>,
426 2012.

427 He, P. Z., Alexander, B., Geng, L., Chi, X. Y., Fan, S. D., Zhan, H. C., Kang, H., Zheng, G. J., Cheng, Y.
428 F., Su, H., Liu, C., and Xie, Z. Q.: Isotopic constraints on heterogeneous sulfate production in Beijing
429 haze, *Atmos. Chem. Phys.*, 18, 5515-5528, <https://doi.org/10.5194/acp-18-5515-2018>, 2018.

430 He, X., Wu, J. J., Ma, Z. C., Xi, X., and Zhang, Y. H.: NH₃-promoted heterogeneous reaction of SO₂ to
431 sulfate on α-Fe₂O₃ particles with coexistence of NO₂ under different relative humidities, *Atmos.*
432 *Environ.*, 262, 118622, <https://doi.org/10.1016/j.atmosenv.2021.118622>, 2021.

433 Holt, B.D. and Kumar R.: Oxygen-18 study of high-temperature air oxidation of SO₂, *Atmos. Environ.*,
434 18, 2089-2094, [https://doi.org/10.1016/0004-6981\(84\)90194-X](https://doi.org/10.1016/0004-6981(84)90194-X), 1984.

435 Huang, R. J., Zhang, Y., Bozzetti, C., Ho, K. F., Cao, J. J., Han, Y., Daellenbach, K. R., Slowik, J. G.,
436 Platt, S. M., Canonaco, F., Zotter, P., Wolf, R., Pieber, S. M., Brun, E. A., Crippa, M., Ciarelli, G.,
437 Piazzalunga, A., Schwikowski, M., Abbaszade, G., Schnelle-Kreis, J., Zimmermann, R., An, Z., Szidat,
438 S., Baltensperger, U., El Haddad, I., and Prevot, A. S.: High secondary aerosol contribution to
439 particulate pollution during haze events in China, *Nature*, 514, 218-222,
440 <https://doi.org/10.1038/nature13774>, 2014.

441 Kuang, B., Zhang, F., Shen, J., Shen, Y., Qu, F., Jin, L., Tang, Q., Tian, X., and Wang, Z.: Chemical
442 characterization, formation mechanisms and source apportionment of PM_{2.5} in north Zhejiang Province:
443 The importance of secondary formation and vehicle emission, *Sci. Total. Environ.*, 851, 158206,
444 <https://doi.org/10.1016/j.scitotenv.2022.158206>, 2022.

445 Li, J. H. Y., Zhang, Y. L., Cao, F., Zhang, W., and Michalski, G.: Stable Sulfur Isotopes Revealed a
446 Major Role of Transition-Metal Ion-Catalyzed SO₂ Oxidation in Haze Episodes, *Environ. Sci. Technol.*,

447 54, 2626-2634, <https://doi.org/10.1021/acs.est.9b07150>, 2020.

448 Lin, Y. C., Yu, M., Xie, F., and Zhang, Y.: Anthropogenic Emission Sources of Sulfate Aerosols in
449 Hangzhou, East China: Insights from Isotope Techniques with Consideration of Fractionation Effects
450 between Gas-to-Particle Transformations, *Environ. Sci. Technol.*, 56, 3905-3914.
451 <https://doi.org/10.1021/acs.est.1c05823>, 2022.

452 Liu, M. X., Song, Y., Zhou, T., Xu, Z. Y., Yan, C. Q., Zheng, M., Wu, Z. J., Hu, M., Wu, Y. S., and Zhu,
453 T.: Fine particle pH during severe haze episodes in northern China, *Geophys. Res. Lett.*, 44, 5213-5221,
454 <https://doi.org/10.1002/2017GL073210>, 2017.

455 Liu, T., Clegg, S. L., Abbatt, J. P. D.: Fast oxidation of sulfur dioxide by hydrogen peroxide in
456 deliquesced aerosol particles, *Proc. Natl Acad. Sci. USA.*, 117, 1354-1359,
457 <https://doi.org/10.1073/pnas.1916401117>, 2020.

458 Liu, Y. Y., Wang, T., Fang, X. Z., Deng, Y., Cheng, H. Y., Nabi, I., and Zhang, L.: Brown carbon: An
459 underlying driving force for rapid atmospheric sulfate formation and haze event, *Sci. Total. Environ.*,
460 734, 139415, <https://doi.org/10.1016/j.scitotenv.2020.139415>, 2020.

461 Meng, X., Hang, Y., Lin, X., Li, T. T., Wang, T. J., Cao, J. J., Fu, Q. Y., Dey, S., Huang, K., Liang, F. C.,
462 Kan, H. D., Shi, X. M., and Liu, Y.: A satellite-driven model to estimate long-term particulate sulfate
463 levels and attributable mortality burden in China, *Environ. Int.*, 171,107740,
464 <https://doi.org/10.1016/j.envint.2023.107740>, 2023.

465 Oh, S. H., Park, K., Park, M., Song, M., Jang, K. S., Schauer, J. J., Bae, G. N., and Bae, M. S.:
466 Comparison of the sources and oxidative potential of PM_{2.5} during winter time in large cities in China
467 and South Korea, *Sci. Total. Environ.*, 859, 160369, <https://doi.org/10.1016/j.scitotenv.2022.160369>,
468 2023.

469 Ramanathan, V., Crutzen, P. J., Kiehl, J. T., and Rosenfeld, D.: Aerosols, climate, and the hydrological
470 cycle, *Science*, 294, 2119-2124, <https://doi.org/10.1126/science.1064034>, 2001.

471 Seinfeld, J. H. and Pandis, S. N.: Atmospheric Chemistry and Physics: From Air Pollution to Climate
472 Change, *Phys. Today*, 51, 88-90, <https://doi.org/10.1063/1.882420>, 1998.

473 Shao, J., Chen, Q., Wang, Y., Lu, X., He, P., Sun, Y., Shah, V., Martin, R. V., Philip, S., Song, S., Zhao,
474 Y., Xie, Z., Zhang, L., and Alexander, B.: Heterogeneous sulfate aerosol formation mechanisms during
475 wintertime Chinese haze events: air quality model assessment using observations of sulfate oxygen

476 isotopes in Beijing, *Atmos. Chem. Phys.*, 19, 6107-6123, <https://doi.org/10.5194/acp-19-6107-2019>,
477 2019.

478 Tanaka, N., Rye, D. M., Xiao, Y., and Lassaga, A. C.: Use of stable sulfur isotope systematic for
479 evaluating oxidation reaction pathways and in-cloud scavenging of sulfur dioxide in the atmosphere,
480 *Geophys. Res. Lett.*, 21, 1519-1522, <https://doi.org/10.1029/94GL00893>, 1994.

481 Wang, G. H., Zhang, R. Y., Gomez, M. E., Yang, L. X., Levy Zamora, M., Hu, M., Lin, Y., Peng, J. F.,
482 Guo, S., Meng, J. J., Li, J. J., Cheng, C. L., Hu, T. F., Ren, Y. Q., Wang, Y. S., Gao, J., Cao, J. J., An, Z.
483 S., Zhou, W. J., Li, G. H., Wang, J. Y., Tian, P. F., Marrero-Ortiz, W., Secrest, J., Du, Z. F., Zheng, J.,
484 Shang, D. J., Zeng, L. M., Shao, M., Wang, W. G., Huang, Y., Wang, Y., Zhu, Y. J., Li, Y. X., Hu, J. X.,
485 Pan, B., Cai, L., Cheng, Y. T., Ji, Y. M., Zhang, F., Rosenfeld, D., Liss, P. S., Duce, R. A., Kolb, C. E.,
486 and Molina, M. J.: Persistent sulfate formation from London Fog to Chinese haze, *Proc. Natl. Acad. Sci.*
487 *U.S. A.*, 113, 13630-13635, <https://doi.org/10.1073/pnas.1616540113>, 2016.

488 Wang, W., Liu, M., Wang, T., Song, Y., and Ge, M.: Sulfate formation is dominated by
489 manganese-catalyzed oxidation of SO₂ on aerosol surfaces during haze events, *Nature Communications*,
490 12, 1993, <https://doi.org/10.1038/s41467-021-22091-6>, 2021.

491 Xue, J., Yuan, Z., Griffith, S. M., Yu, X., Lau, A. K. H., and Yu, J. Z.: Sulfate Formation Enhanced by a
492 Cocktail of High NO_x, SO₂, Particulate Matter, and Droplet pH during Haze-Fog Events in Megacities
493 in China: An Observation-Based Modeling Investigation, *Environ. Sci. Technol.*, 50, 7325-7334,
494 <https://doi.org/10.1021/acs.est.6b00768>, 2016.

495 Xue, J., Yuan, Z., Yu, J. Z., and Lau, A. K. H.: An Observation-Based Model for Secondary Inorganic
496 Aerosols, *Aerosol Air Qual. Res.*, 14, 862-878, <https://doi.org/10.4209/aaqr.2013.06.0188>, 2014.

497 Yang, T., Xu, Y., Ye, Q., Ma, Y. J., Wang, Y. C., Yu, J. Z., Duan, Y. S., Li, C. X., Xiao, H. W., Li, Z. Y.,
498 Zhao, Y., and Xiao, H. Y.: Spatial and diurnal variations of aerosol organosulfates in summertime
499 Shanghai, China: potential influence of photochemical processes and anthropogenic sulfate pollution,
500 *Atmos. Chem. Phys.*, 23, 13433-13450, <https://doi.org/10.5194/acp-23-13433-2023>, 2023.

501 Ye, C., Liu, P. F., Ma, Z. B., Xue, C. Y., Zhang, C. L., Zhang, Y. Y., Liu, J. F., Liu, C. T., Sun, X., and
502 Mu, Y. J.: High H₂O₂ Concentrations Observed during Haze Periods during the Winter in Beijing:
503 Importance of H₂O₂ Oxidation in Sulfate Formation, *Environ. Sci. Technol. Lett.*, 5, 757-763,
504 <https://doi.org/10.1021/acs.estlett.8b00579>, 2018.

505 Zhang, R., Sun, X. S., Shi, A. J., Huang, Y. H., Yan, J., Nie, T., Yan, X., and Li, X.: Secondary
506 inorganic aerosols formation during haze episodes at an urban site in Beijing, China, *Atmos. Environ.*,
507 177, 275-282, <https://doi.org/10.1016/j.jes.2022.01.008>, 2018.

508 Zhang, Y., Bao, F. X., Li, M., Xia, H. L., Huang, D., Chen C. C., and Zhao, J. C.: Photoinduced Uptake
509 and Oxidation of SO₂ on Beijing Urban PM_{2.5}, *Environ. Sci. Technol.*, 54,
510 14868-14876, <https://doi.org/10.1021/acs.est.0c01532>, 2020.